SAFETY EVALUATION AND RESEARCH ON FRACTURE THREAD JOINT BASED ON FINITE ELEMENT CALCULATION AND SCANNING ELECTRON MICROSCOPY

Ning Tingzhou, Zhang Jingzhi*
College of Mechanical and Electrical Engineering, Zaozhuang University, Zaozhuang, China
E-mail:zjzsd2003@163.com

***ABSTRACT**: This paper makes an in-depth study on the fracture of the drill string connection thread joint, include electron microscope scanning and phase composition analysis, and find that there are serious defects at the internal of thread, there is potential fatigue fracture risk of for threaded joints. According to Farr formula and three–direction stress theory, considering the bending deformation of the drill string into the actual well hole, do the finite element simulation of stress state of thread joint, and find the stress of the connection thread part reaches the ultimate load of the material. Finally, through the safety evaluation, analysis of stress concentration factor and notch fatigue sensitivity coefficient, and the internal defect of thread joint material affecting the crack extension at the notch is available. In addition, the maximum stress occurs at bottom of the first tooth which accords with the actual fracture location. Comprehensive analysis reveals that the effect of cyclic bending load and internal defect of thread that leads to fatigue failure of connection thread and fracture.*

KEYWORDS: Electron microscope scanning; Composition analysis; Thread joint; Safety evaluation

1 INTRODUCTION

Oil well tubing is widely used in the well test, fracture acidizing, water injection, oil production etc. underground work, it is the major force and power transmission components of oil well operation and production. In extended reach well and high angle deviated hole, oil well tubing mechanics behavior research has become one of the key problems to be solved[1,2].

When the string passes through curved section, bending deformation will lead to stress concentration at string shell. For this reason, some scholars and experts at home and abroad carried out researches on the fracture failures of threaded connection. Zhang J et al conducted failure analysis of the string with FEM, and carried out reliability evaluation of API thread of pipe joint and experimental study on stress field of thread button in the processing of make-up [3-5]. During the inevitable working condition of rotating and bending, API stress-relief grooves cannot fundamentally solve the fatigue fracture problem, its stress concentration factor and notch sensitivity factor are very high [6-8]. Domestic and international scholar interested on the issue of drilling tools material itself, and studying how the stress concentration factor and notch sensitivity factor changing with different of thread structure[9-11]. Tomoya Inoue, et al pointed out many joints appear fatigue crack at first in the last engaged threads, following with crack propagation, and leading to piercing or fracture at last, which providing theoretical basis for modifying the joint of drilling tools and improving their anti-fatigue life [12-14].

On the basis of previous studies, this paper studies the fracture failure of special thread connection, and drown lessons from foreign scholars on the fracture analysis method [15,16], in addition, carried out the safety evaluation of special thread connection, which provided an effective way to judge the fatigue crack growth of the thread under the condition of stress concentration.

2 STRUCTURE AND WORKING PRINCIPLE OF PDM

PDM positive displacement motor (abbreviation PDM) drill has become the most widely used downhole tool in oil drilling engineering. As shown in Fig.1, the PDM is made of four major components, i.e., outlet valve assembly, motor assembly, cardan shaft assembly and drive shaft assembly. In the working process of the PDM, the stator is fixed, and the rotor is driven by the high-pressure drilling fluid to move around the axis of the stator. The cardan shaft assembly transmits the planetary motion to the drive shaft and the drive shaft drives PDC bit to rotate. When drilling in or circulating drilling fluid, the outlet valve is closed

and the drilling fluid enters into the motor. The PDM is the tool that converts hydraulic energy of the drilling fluid into mechanical energy of bit, which breaks the rock and drills in.

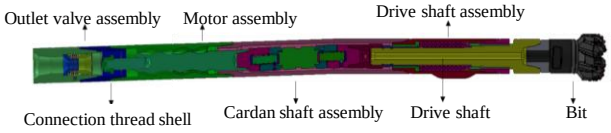

Fig. 1 3D visualization graphic of positive displacement motor

It is about range of 1420-1433m in the well hole and at last 70.5min, the torque values fluctuate in the range of 7-16kN· m, which is at 5-7min/m in the drilling process, which is the normal drilling of the well section. The depth of combine drilling is about at 1433.59m, pump pressure from the initial 18-19Mpa suddenly rose to 25Mpa, then turn off the pump and heave the string upwards immediately, single pump circulation and maintains pump pressure at 15Mpa, and cannot arrive the bottom, which can judge downhole anomaly, after drawing out the drill string and find the connection thread broken down in the well, the specific working parameters of the drill string are shown in Table 1.

Fig.2 Fracture of cardan shaft shell in the oil field

Table 1 Usage record of the drill string

Number	Well section/m	Drilling press/T	Torque/ kN • m	Using time/ hour
1	1040-1047	8-10	12-20	43
2	1047-1593	12-14	14-21	35
3	1160-1433	12-15	15-21	52

We could also find the fracture connection thread from Fig.2, the stress distribution of drill string is complex in the rotary and direction drilling process, so the stress of tensile, bending was one of the important factors, and twisting is an important factor in the wear and failure of drilling tool joints leading to failure.

3 FRACTURE ANALYSIS

3.1 Fracture macroscopic inspection analysis

Through checking the connecting threads, the fracture position was corresponding to location of the first tooth. The profile of fracture was a flat vertical section, where the clearance of top and bottom of two teeth was large, and fracture along 45 ° direction, more than one-second of the fracture range showed the characteristics of shear failure, as shown in Fig.3.

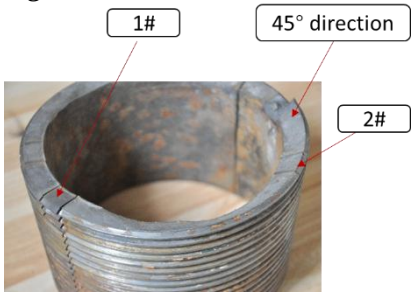

Fig. 3 Dispositon and number of cracks

3.2 Scanning electron microscopy analysis of fracture

Scanning electron microscopy of the 1# sample: it is found that there was obvious tearing trace near the bottom of thread. According to this, we could judge the crack initiation site is mainly composed of dimples, the middle part of the crack and the quasi cleavage of the tail, which showed that there was a certain brittleness in the area as shown in Fig.4.

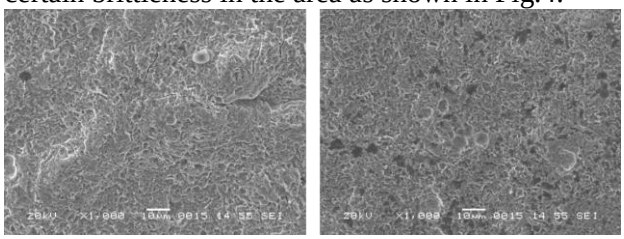

Fig. 4 Quasi cleavage morphology and dimples in the 1# crack surface

Scanning electron microscopy of the 2 # sample: the fracture surface has been worn in a large area, there are a large number of micro cracks on the joint surface of the cone, and the fracture plane there was a clear large dimple morphology area on the tail of crack, which proved its earlier break as shown in Fig.5.

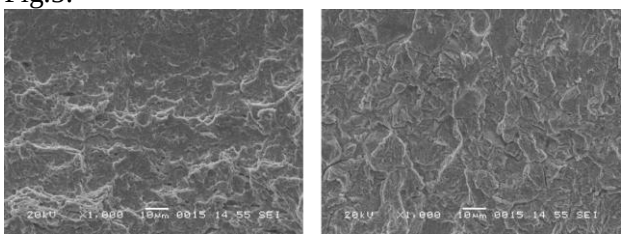

Fig. 5 Quasi cleavage and dimple morphology area in the 2# crack surface

3.3 Phase composition analysis of fracture

As shown in Fig.6, specimen 1# has no over standard inclusions (there is a 0.05mm long undeformed inclusion), there is a 0.1mm long crack along the fracture edge with a gray matter (about

0.03mm long) as shown in Fig.6 (a), there is a 0.15mm long crack at the root edge of the thread, and there is no abnormal structure on both sides of the crack. The microstructure of 1# samples are sorbite and ferrite as shown in Fig.6 (b).

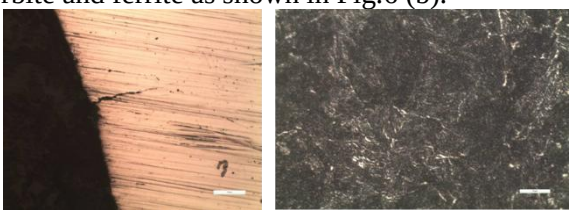

(a) (b)

Fig. 6 Optical micrographs and Compositional tissue fractograph of specimen 1#

As shown in Fig.7, there are no inclusions exceeding the standard in specimen 2# [17], and there are several notches on the outer layer of the root edge of the thread beside the fracture (the deepest part is about 0.12mm) as shown in Fig. 7(a). The microstructure of 2# samples are sorbite and ferrite as shown in Fig.7 (b).

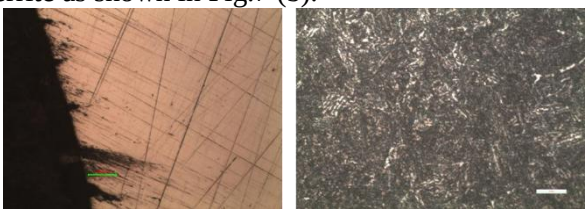

(a) (b)

Fig. 7 Optical micrographs and Compositional tissue fractograph of specimen 2#

The following conclusions can be obtained by means of metallographic observation and composition analysis:

1）1# and 2# crack metallographic observation two crack depth is bigger, the depth of 1# crack is 0.78-1.38mm, the depth of 2# crack is1.0-1.5mm. If there is no rapid extension and fracture, connection thread will also likely to break from 1# and 2# crack. Just because the main crack is weaker and priority to destruction, in addition, the stress release is focused on this position, which cause 1# and 2# cracks stop to expanding, and it is also proved that 1# and 2# crack are not the main crack secondary crack, but the initiation time is similar to the main crack.

2）There is no oxidation or decarburization layer from the 1#, 2# cracks metallographic observation（It is possible that the thread is cut off, but the possibility is very small）. Two cracks are only along the base of tooth, it is not extended to the teeth lateral side or teeth top, which is consistent with the stress concentration, however, the crack propagation of heat treatment is random. Therefore, it is possible to exclude the possibility of heat treatment.

3.4 Chemical composition analysis

The fracture surface of thread joint of cardan shaft shell in Fig.3 is sampled for material testing. The chemical composition of cardan shaft shell is tested and analyzed by using HCS-140 high frequency infrared sulfur carbon analyzer. It can be found that the composition of cardan shaft shell sample mainly includes 12 elements through Inductively Coupled Plasma atomic emission spectrometer（ICP-AES）, such as C, Si, Mn, P, S, Ni, Cr, Mo, Cu, N, O, H, as shown in Table 2. It can be found from the test results that the contents of harmful elements S and P are controlled within the standard allowable ranges [18].

Table 2 Test results of chemical composition (wt%)

Element	C	Si	Mn	S	P	Cr
Standard	0.38 ~0.43	0.20 ~0.37	0.60 ~0.80	≤ 0.015	≤ 0.015	1.00 ~1.20
Detection (1#)	0.43	0.24	0.65	0.0093	0.013	1.01
Detection (2#)	0.42	0.22	0.67	0.0072	1.02	1.02

Element	Mo	Ni	Cu	O	N
Standard	0.17~0.25	≤ 0.30	≤ 0.20	≤ 0.0015	≤ 0.008
Detection (1#)	0.2	0.032	0.084	0.0009	0.002
Detection (2#)	0.21	0.031	0.086	0.001	0.0025

3.5 Mechanical properties test

A 200 mm specimen was sectioned from the cardan shaft shell close to 10 mm from the fracture, and it's tensile and impact mechanical properties are tested.

Tensile Standard for 40CrMo Specimens: Tensile strength (≥1080 MPa), yield strength (≥830 MPa), fracture elongation (≥ 12%), reduction of area (≥ 45%) and impact toughness (≥ 63J/cm2) all meet the standard requirements as shown in Table 3 and Table 4. The tensile test result is lower than the standard requirements, and the impact energy of impact test meets the standard requirements [19].

Table 3 Tensile properties of the shell

Number	Tensile strength (MPa)	Yield strength $Rp_{0.2}$(MPa)	Max force KN	Fracture elongation δ (%)	Reduction of Area ψ(%)
1#	999	813	78.6	14.5	53
2#	1008	824	79.0	15.0	51
3#	1016	841	79.7	14.0	52
4#	986	798	77.3	14.5	54
5#	995	808	78.2	14.0	54

Table 4 Test results of Charpy impact test

Number	Pre-notched	Impact energy/ Wt(J)	Impact toughness/Ak (J/cm^2)
1	U	79	92.3
2	U	60	74.3
3	U	60	82.1
4	U	52	69.5
5	U	60	78.4
6	U	79	92.1

4 FINITE ELEMENT MECHANICAL MODEL OF SPECIAL CONNECTION THREAD

4.1 Judgment criteria of the strength of the thread

Based on the structure and dimensions of special connection thread developed, the finite element mechanical model of special connection thread, in the model, contact pressure after thread on is suffered by external shoulder plane. The contact pressure is P . Their value can be calculated by Farr formula, given by (1), which is recommended by API RP7G standards [9].

$$P = \frac{12T_n}{\left[\frac{h}{2\pi} + \frac{R_t f}{\cos\theta} + R_S f\right]} \quad (1)$$

Where, P is contact pressure between the shoulders kN , T_n is make up torque, $kN \cdot m$, h is thread pitch, mm. R_t is average radius of thread, mm. f is friction coefficient among the connection shoulder. R_s is connection shoulder average radius, mm. θ is thread half angle, °.

Thread connection also need to follow the fourth strength theory, and definition of yield strength of Von Mises (the fourth strength theory) could also be written:

$$\sqrt{\frac{1}{2}\left[(\sigma_1-\sigma_2)^2+(\sigma_2-\sigma_3)^2+(\sigma_3-\sigma_1)^2\right]} = \sigma_s \quad (2)$$

or

$$\sigma_1 - \sigma_3 = \sqrt{\sigma^2 + 3\tau^2} \le [\sigma_s] \quad (3)$$

Among them, σ_1 is the first principal stress, σ_s is the limiting value for yield strength and σ_3 is the third principal stress.

4.2 Calculation model of the special thread

The material of the threaded connection is 42CrMo, the elastic modulus E of which is 206,000, Poisson's ratio is 0.3, yield stress σ_s is 945 MPa, tensile strength σ_b is 1020 MPa, and coefficient of friction is 0.12. Based on the above structure and material properties, the isotropic bilinear elastic–plastic material model may be established. The C3D8R octahedral element is used for meshing the model, and for the reasonable refinement of the element at the thread turns. The finite element mesh and design model are shown in Fig. 9 and Fig. 10. Loading conditions: fixed constraints are applied at one end of the thread, and make-up torque and bending moment are loaded at the other end.

Fig.9 Matching model of special thread teeth

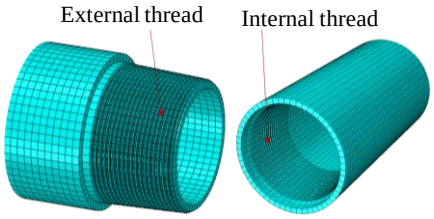

Fig.10 Finite Element Model of special connection thread

4.3 The analysis of calculation results

According to Farr formula and the fourth strength theory, it is mainly obtained three-dimensional stress through the finite element calculation. According to the data provided on site and the size of thread, the three direction Von Mises stress (S11, S22, S33) is obtained under bending load as shown in Fig. 11. The range of larger stress was 250-1068MPa, among them, the value of S11 is the largest, which is 1068 MPa, this value is the limited stress load, and it was easy to occur stress concentration and fatigue crack in this position.

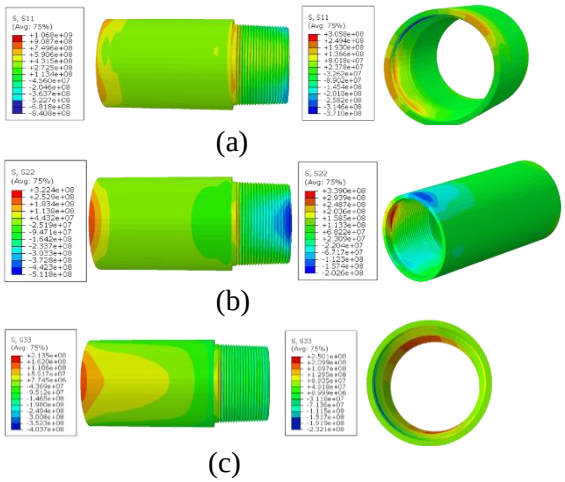

Fig. 11 Von Mises three direction stress contour

According to the analysis, it was found that Von Mises stress of internal thread and external thread in

the curvature of S22 and S33, which were far less than the yield strength of material, but the change of S11 was relatively larger. In addition, this paper studied the Von Mises stress curve of thread under the curvatures well hole. Fig. 12 is the S11, S33 and S22 of the first tooth in the circumferential direction of teeth, the stress changes from small to large and then from large to small. The average stress change of two teeth is not different. The S33of the first tooth in the circumferential direction of teeth, the stress changes from small to large and then from large to small, the average stress change of two teeth is not different. Relative to S11 and S22, stress values of S33 have a stable period, and the change of the first tooth stress was almost the same as that of the second teeth.

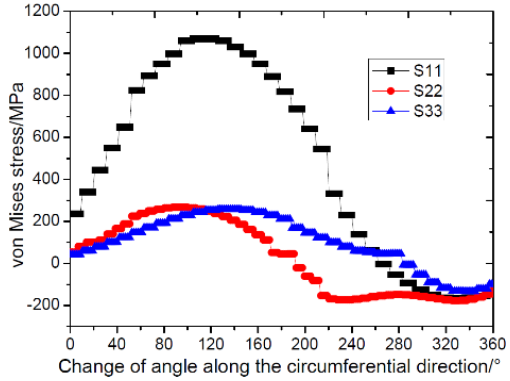

Fig.12 Three direction stress curve of external thread under action of curvature

When a certain shear stress in the material reaches the maximum value, the material will yield, as shown in the Fig.13, when the first tooth reach the shear stress of nearly 1000MPa under the bending load, the material will yield and finally failure.

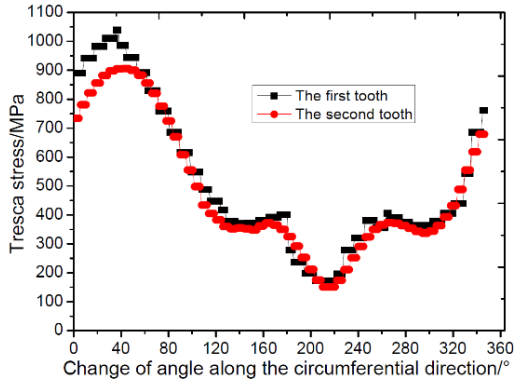

Fig.13 Tresca stress curve of external thread under action of curvature

The contact pressure of thread section from the following Fig.14 and Fig.15, it is found that the contact pressure of the first tooth exceeds the allowable stress of the material, where is the most destructive position and the actual last breakout place.

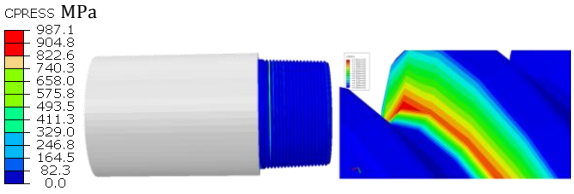

Fig.14 Contact pressure contour of external thread

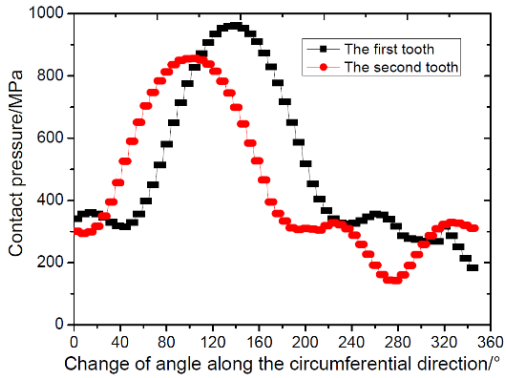

Fig.15 Contact pressure curve of the two teeth

Combined to the contour and curve of three direction stress under three kinds of curvature, it was found that the displacement of internal and external thread increased gradually along the axis direction of thread.

5 SAFETY EVALUATION OF SPECIAL THREAD CONNECTION

5.1 Analysis of stress concentration factor and notch fatigue sensitivity coefficient

Notch stress concentration factor K_t is defined as the radio between the maximum local elastic stress σ_{max} and the nominal stress σ_0, shown in equation (4). However, for a simple thread structure, K_t can be obtained by equation (5).

$$K_t = \frac{\sigma_{max}}{\sigma_0} \tag{4}$$

$$K_t = 1 + 2\sqrt{\frac{t}{\rho}} \tag{5}$$

Where, K_t is the stress concentration factor, t is depth of tooth, ρ is fillet radius of connection root

However, for some complicated thread structure, K_t can be calculated by equation (4), which σ_{max} could be obtained by finite element analysis method.

Stress concentration has a significant impact on fatigue strength [13]. However, it is not enough to depict the impact only by the theoretical stress concentration coefficient. Some researchers put

forward fatigue notch sensitive coefficient K_f, which presents that a coefficient of notch affects fatigue strength, also known as fatigue stress concentration coefficient or deterioration of fatigue strength coefficient. It can be calculated by equation (6).

$$K_f = \frac{S_e}{S_w} \qquad (6)$$

Where, S_e is the fatigue strength of smooth sample, S_w is the fatigue strength of notch sample.

Experimental study shows that, material plastic property is one of main reason for affecting fatigue notch sensitive coefficient K_f. A material with good ductility, K_f is much less than K_t, which means fatigue strength is insensitive to notch. However, for brittle materials, K_f is close to K_t, that means fatigue strength is sensitive to notch. Based on the model of average stress, R.E. Peterson assumed stress decreased linearly inwards from notch position, shown in Fig. 16.

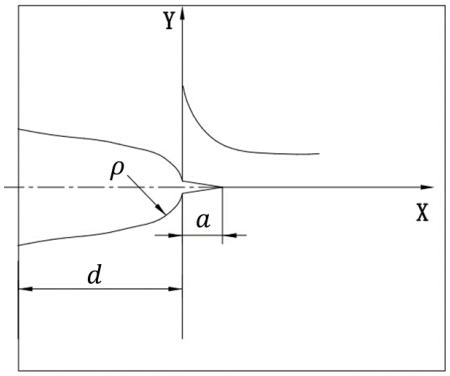

Fig.16 Sketch diagram of thread notch

Considering lower stress material bracing effects on high stress material, fatigue damage occurred when average stress of notch root a position equal to or more than fatigue strength of smooth sample. The relationship between K_f and K_t is shown as equation (7).

$$K_f = 1 + \frac{K_t - 1}{1 + \frac{a}{\rho}} \qquad (7)$$

Where, ρ is radius of notch root, a is material constant, for quenched and tempered steel a =0.635 mm, and for normalizing steels a =0.254 mm.

Stress concentration coefficient of simple thread structure can be obtained by equation (5), in theory. However, actually threads structure of drilling tools joint is very complex in petroleum industry. Their notch stress concentration coefficient K_t cannot be calculated by equation (5) anymore. Therefore, in this paper, we first get the maximum stress of threads notch σmax by the method of finite element. Then, their stress concentration coefficient is obtained by equation (4). Finally, their fatigue notch sensitive coefficient is got by equation (7).

5.2 Damaging test experimentation

The connection thread is easy to be scratched in the process of normal disassembly as shown in Fig. 17, which will cause the teeth to be miss and scratched.

Fig.17 The teeth missing and scraching

6 CONCLUSION

Based on the relevant theories, field data and experimental results, some conclusions and knowledge are available as follows:

1) Through scanning electron microscopy and phase composition analysis of fracture, it is found that there is material defect at thread fracture, moreover, micro cracks are blunted through bifurcation, which lead to the crack growth rate decreases. It can be exclude the cause of heat treatment, we could judge the source area of crack fracture through these results.

2) This will add to the thread part of a quenching and tempering treatment, it is bound to affect the crystal structure of the thread, and there is no standard specification for fastening and disassembly process will cause the thread of the buckle, lack of teeth, squeezing, and affect the life of connection thread inevitably

3) In the normal drilling and stopping process, there is no human factor in the operation and use of errors, the material strength of connection thread of the string is within a reasonable range, the results of experimental tests and finite element analysis show that the material has begun to yield, and then subjected to underground vibration, bending, torsion, compression and other composite load, it is necessary to form the fatigue crack from the maximum stress interval.

4) The finite element calculation of the motion state of the drill string in the 3D well, the results of

Von Mises three direction stress prove that the stress state of the connection thread is consistent with the fourth strength theory and Farr formula.

5) It is find that lower stress material bracing effects on high stress material, fatigue damage occurred when average stress of notch root a position equal to or more than fatigue strength of smooth sample. Therefore, the correctness of the formula of stress concentration factor and notch fatigue sensitivity coefficient of connection thread is verified.

ACKNOWLEDGEMENTS

This work was supported by Zaozhuang Science and Technology Plan Project (2019GX10) and Zaozhuang University Doctoral Research Startup Fund Project (2018BS030).

REFERENCES

- Huang Yun, Liu Qingyou, et al. A study on mechanical model of the three dimensional curved hole on energy method [J] .Drilling and Production Technology, 35(5), 2012: 80－82.
- Petroleum and natural gas industries-drilling and production equipment-Part 1: Drill stem design and operating limits, ISO/CD 10407-1, 2004-04-21.
- Jie Zhang, Zheng Liang, Chuanjun Han. Failure analysis and finite element simulation of key components of PDM Engineering Failure Analysis. 2014 Vol. 45(7):15-25.
- LIN Teng-jiao, LI Run-fang, XU Ming-yu. Numerical Simulation of Elastoplastic Contact Characteristic for Drillpipe Thread Compounds with Two Steps. Machine Design and Research 20（2004), 48-49.
- LIN Yuan-hua, SH I Tai-he, YAO Zhen-qiang. A Model to Compute the Mechanical Property of Drillpipe Tool Joint and Its Application. Journal of Shanghai Jiaotong University, 2005, 39(7): 1058-1062.
- ZHU Xiao-hua, SHI Chang-shuai, TONG Hua. Optimizing loading path and die line type of large length-to-diameter ratio metal stator screw lining hydroforming [J]. Journal of Central South University, 2015, 22:224-231.
- WANG Xin-hu, XUE Ji-jun, GAO Rong. Study on longitudinal fracture mechanism and material property indicators of Box-ended drill pipe tool joint. NATURAL GAS INDUSTRY, 2007, 27(4):69- 71.
- Han, Sungkon, Knight, Matthew, Brennan, Fergal P, et al. Fatigue analysis of drillstring threaded connections[C]. The International Society of Offshore and Polar Engineers, 2003. Honolulu, Hawaii.
- Michael Jellison, R. Brett Chandler, et al. Deepwater and Critical Drilling With New Connection Technology—Case Histories and Lessons Learned. SPE 133857, at the SPE Asia Pacific Oil & Gas Conference and Exhibition held in Brisbane, Queensland, Australia, 18–20 October 2010.
- Guillaume Plessis, and Jim Brock, et al. Successful Implementation of Latest Generation of Double Shoulder Connection Technology in Fast Slimhole Drilling – A Review after Broad Adoption in the Gulf of Thailand. IADC/SPE 156423, at the IADC/SPE Asia Pacific Drilling Technology Conference and Exhibition held in Tianjin, China, 9–11 July 2012.
- C.Santus, L.Bertini, M.Behini, et al. Torsional Strength Comparison between Two Assembling Techniques for Aluminium Drill Pipe to Steel Tool Joint Connection [J]. International journal of pressure vessels and piping. 2009, 86:117-186.
- Tomoya Inoue, Koji Sakura and Toshihiko Fukui. Fatigue Strength Evaluation of Drill Pipe for Challenging Scientific Drilling Operations. IADC/SPE-170539-MS, at the IADC/SPE Asia Pacific Drilling Technology Conference held in Bangkok, Thailand, 25–27 August 2014.
- O. Vaisberg1, O. Vincké1, G. Perrin et al. Fatigue of Drill string State of the Art [J], Oil & Gas Science and Technology. 2002, 57(1): 7-37.
- A.R. Shahani, S.M.H.Sharifi. Contact stress analysis and calculation of stress concentration factors at the tool joint of a drill pipe [J]. Material and design. 2009, 30, 3615-3621.
- S.E. Moussavi Torshizi, M. Ebrahimi. Failure analysis of gas turbine transition pieces, leading to a solution for prevention. Engineering Failure Analysis 32 (2013) 402–411.
- A. Mokaberi, R. Derakhshandeh-Haghighi, Y. Abbaszadeh. Fatigue fracture analysis of gas turbine compressor blades. Engineering Failure Analysis 58 (2015) 1–7.
- GB/T 10561-2005 Steel-Determination of content of nonmetallic inclusions Micrographic method using standards diagrams[S].

- GB/T 222-2006 Permissible tolerances for chemical composition of steel products [S].
- GB/T 228.1-2010 Metallic materials-Tesile testing-Part 1: Method of test at room temperature [S].